Study of $h\gamma Z$ coupling using $e^+e^- \to h\gamma$ at the ILC

Yumi Aoki[1], Keisuke Fujii[2], Sunghoon Jung[3], Junghwan Lee[3], Junping Tian[4], Hiroshi Yokoya[5]
on behalf of the ILD concept group

SOKENDAI[1], KEK[2], Seoul National University[3],University of Tokyo[4], KIAS[5]

February 5, 2019

Abstract

We study the $e^+e^- \to h\gamma$ at the International Linear Collider (ILC) to probe new physics in $h\gamma Z$ coupling. The study is performed at center mass energies of 250 GeV based on the full simulation of the International Large Detector (ILD). As a result, with an integrated luminosity of 2000 fb^{-1} the significance for standard model $e^+e^- \to h\gamma$ process is 0.53 σ. We give the 95 % confidence level upper limit for its cross section 1.08 fb for left handed beam polarization case.

This study was performed in the framework of the ILD concept. Talk presented at the International Workshop on Future Linear Colliders (LCWS2018), Arlington, Texas, 22-26 October 2018. C18-10-22.

1 Introduction

The discovery of the Higgs boson at the Large Hadron Collider (LHC) has completed the standard model particle spectrum. The most important task is now to find physics beyond the standard model. Precision study of the Higgs boson is a powerful tool for this purpose. The International Linear Collider (ILC) [1] is an ideal machine to carry out the precision Higgs measurements.

The motivation of our study is to find new physics effects in $h\gamma\gamma$ and $h\gamma Z$ couplings. Since these couplings appear only at the loop level in the standard model, they are potentially very sensitive to new physics and being studied at the LHC. As one example, the expected deviations on $e^+e^- \to h\gamma$ cross section and $h \to \gamma\gamma$ branching ratios in the Inert Doublet Model [2] are shown in Figure 1, which suggests that depending on model parameters the deviations can be as large as 100%.

An usual method to measure $h\gamma\gamma$ and $h\gamma Z$ couplings is to use decay branching ratios of $h \to \gamma\gamma/\gamma Z$. It is, however, very challenging to measure the $h \to \gamma Z$ branching ratio even at the HL-LHC: only a 3σ significance is expected. As a complementary method we study these couplings in a production process at the ILC, $e^+e^- \to h\gamma$ (see Figure 2).

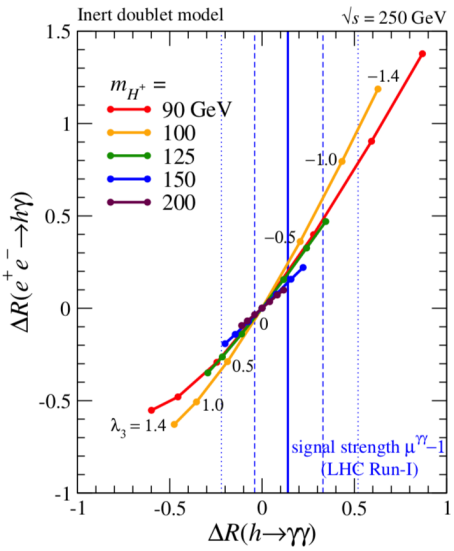

Figure 1: The relative deviations of the $e^+e^- \to h\gamma$ cross section and the $h \to \gamma\gamma$ branching ratio with respect to the Standard Model values [2]

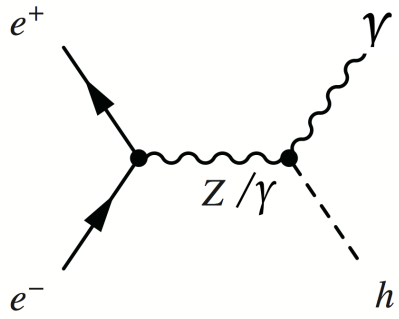

Figure 2: The Feynman diagram of $e^+e^- \to h\gamma$

In addition, the $h\gamma Z$ coupling appears in an s-channel photon exchange diagram for the leading single Higgs production process: $e^+e^- \to hZ$ in the effective field theory framework. It is hence necessary to know the contribution from this diagram. Furthermore, it turns out that the anomalous $h\gamma Z$, $h\gamma\gamma$, hZZ, and hWW couplings come from a common set of a few dimension-6 operators, hence the measurement of the $h\gamma Z$ coupling using $e^+e^- \to h\gamma$ has a potential to provide one very useful constraint on those operators.

In section 2, we introduce the theoretical framework. In section 3, we introduce the experimental method and simulation framework. In section 4, we present the event selection and analysis result.

2 Theoretical Framework

In this analysis, we use the effective Lagrangian shown in Equation 1 to include new physics contributions to the $e^+e^- \to h\gamma$ cross section model-independently,

$$\mathcal{L}_{h\gamma} = \mathcal{L}_{\mathrm{SM}} + \frac{\zeta_{AZ}}{v} A_{\mu\nu} Z^{\mu\nu} h + \frac{\zeta_A}{2v} A_{\mu\nu} A^{\mu\nu} h, \tag{1}$$

where ζ_{AZ} and ζ_A terms represent respectively effective $h\gamma Z$ and $h\gamma\gamma$ coupling from new physics. $A_\mu\nu$, and $Z\mu\nu$ are field strength tensors. v is the vacuum expectation value. The first term is the Standard Model Lagrangian. The three terms contribute to e^+e^- $toh\gamma$ process via the Feynman diagrams shown in Figure 3, where the first SM diagram represents several loop induced diagrams as shown in Figure 4.

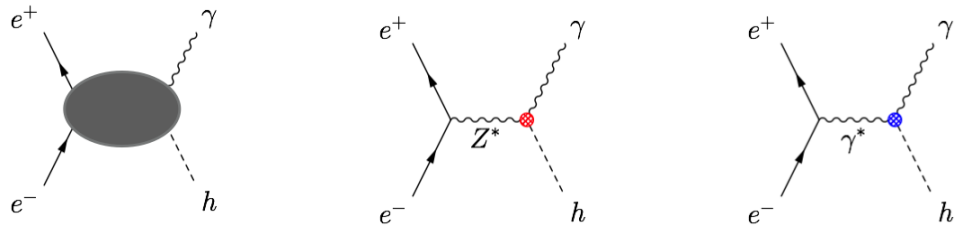

Figure 3: The diagram each terms of Equation 1

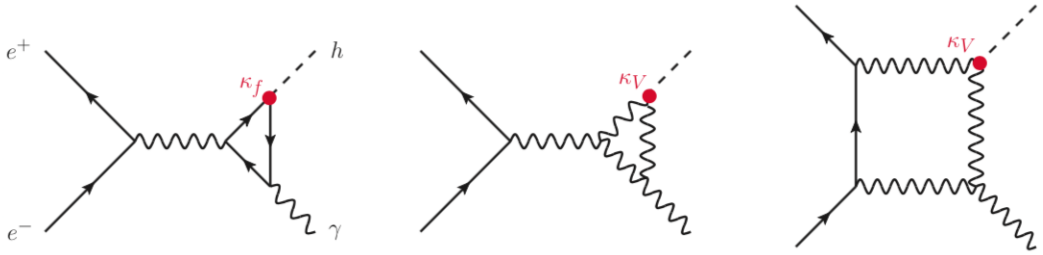

Figure 4: The loop induced Feynman diagrams in Standard Model for $e^+e^- \to h\gamma$ [2]

The SM cross sections at $\sqrt{s} = 250$ GeV are calculated as shown in Table 1. The cross section including effective $h\gamma Z/h\gamma\gamma$ couplings from new physics are calculated as in $P(e^-, e^+) = (+100\%, -100\%)$) , up to interference term.

$$\frac{\sigma_{\gamma H}}{\sigma_{SM}} = 1 - 201\zeta_A - 273\zeta_{AZ} \tag{2}$$

$$\frac{\sigma_{\gamma H}}{\sigma_{SM}} = 1 + 492\zeta_A - 311\zeta_{AZ} \tag{3}$$

Table 1: SM cross sections for different beam polarizations ($\sqrt{s}$ = 250 GeV)

P_{e^-}	P_{e^+}	σ_{SM}[fb]
-100%	+100%	0.35
+100%	-100%	0.016
-80%	+30%	0.20

3 Experimental Method and Simulation Framework

3.1 Experimental Method

In order to determine both ζ_{AZ} and ζ_A, we need two measurements. There are two strategies:
1. Measure the cross sections of $e^+e^- \to \gamma h$ for two different beam polarizations.
2. Since ζ_A can be constrained already by measurement of $h \to \gamma\gamma$ branching ratio at LHC, we can determine $\zeta_A Z$ parameter by just measuring cross section of $e^+e^- \to h\gamma$ for one single polarization.

3.2 Simulation framework

We use fully-simulated Monte-Carlo (MC) samples with the ILD detector model [4]. For event generators, we use Physsim [5] for signal, and we use Whizard [6] for background. We use Mokka [7] based on Geant4 [8] for detector simulation, and use Marlin in iLCSoft [9] for event reconstruction, where particle flow is based on PandoraPFA [10] and flavor tagging is based LCFI+ [11]. The analysis is done for $\sqrt{s}$=250 GeV, assuming Integrated Luminosity of 2000 fb^{-1}.

4 Event selection and Results

4.1 Event selection

The signal channel studied in this paper is $e^+e^- \to h\gamma$, followed by $h \to b\bar{b}$. In the final states of signal events, there are one isolated monochromatic photon with energy 93 GeV, and two b jets with invariant mass consistent with Higgs mass. The main background would be $e^+e^- \to \gamma q\bar{q}$, dominated by $e^+e^- \to \gamma Z$.

As pre-selection, we start with identifying one isolated photon with energy greater than 50 GeV. The split photon clusters within a small cone are recovered. The particles other than the photon are clustered into two jets using Durham algorithm.

In the final selection. The first cut is applied to require the two jets are b-jets. Figure 5 shows the distribution of b likeliness, defined as the larger b-tag among the two jets, for signal and background events with unit normalization. We require b likeliness greater than 0.77 to suppress the light flavor $\gamma q\bar{q}$ events. The cut value is optimized to maximize the

signal significance defined as

$$\text{significance} = \frac{N_s}{\sqrt{N_s + N_B}} \tag{4}$$

where N_s and N_B are number of signal and background events respectively.

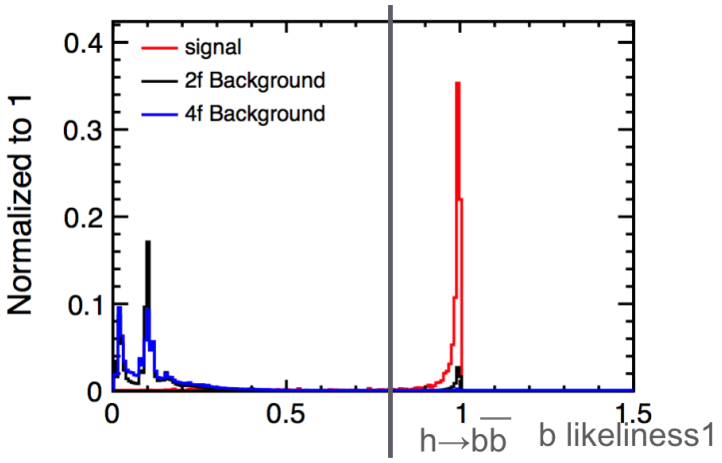

Figure 5: The distribution of b likeliness for signal and background events with unit normalization

The second cut is applied to require that there is not much missing energy. Figure 6 shows the distribution of missing energy. We require missing energy less than 35 GeV.

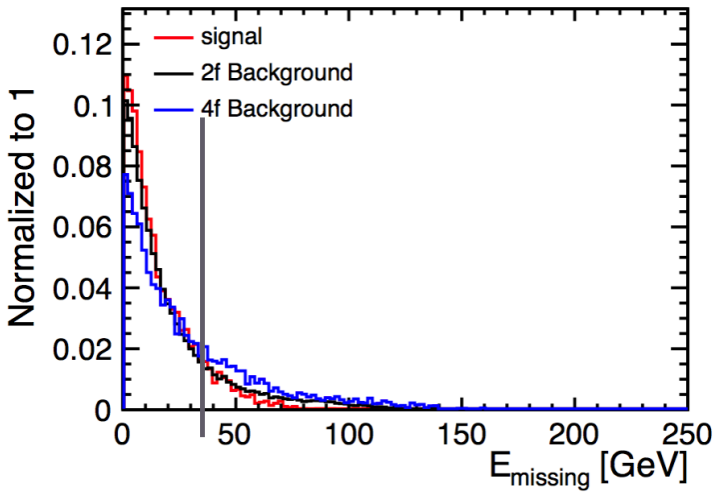

Figure 6: The distribution of b missing energy for signal and background events with unit normalization

As a final cut, we used Multivariate Analysis method. A BDT is trained using 5 input variables based on TMVA [12]: the Higgs invariant mass, Energy of photon, Polar angle of

photon, Smaller angle between photon and a jet, Angle between 2 jets. Figure 7 illustrate these input variables. Figure 8 shows the distributions of each input variable for signal and background events. The blue histograms are for signal events, and the red histograms are for background events. A final cut is applied that the BDT output is greater than 0.0126.

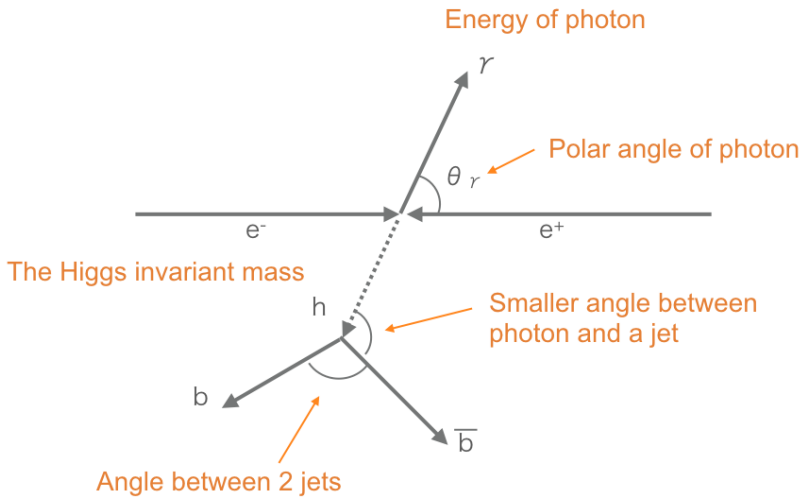

Figure 7: The input variables for TMVA

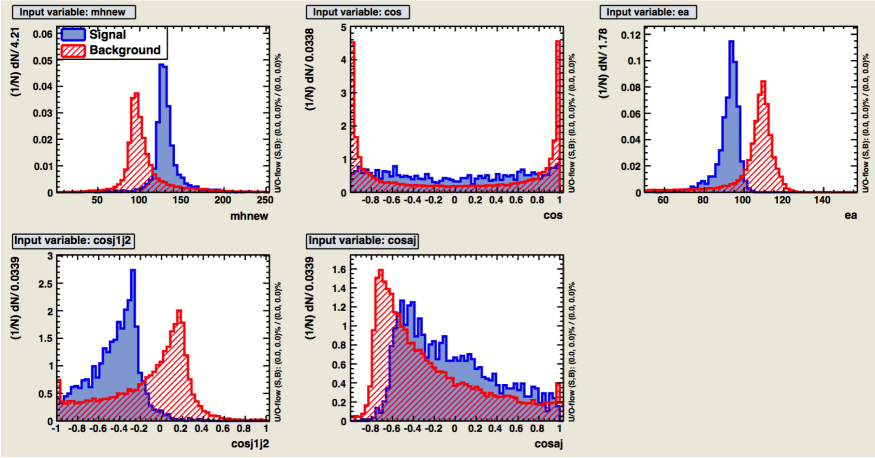

Figure 8: The distributions of TMVA input variable for signal and background.

Figure 9 shows the distribution of $m(b\bar{b})$ after all the other cuts for the signal and background events normalized to an integrated luminosity of 2000 fb^{-1} for the left-handed beam polarization. The remained background events are dominated by $2f$ processes.

4.2 Result

Table 2 gives the number of signal and background events, as well as the signal significance after each cut. The significance is defined Equation 4. After all the cuts, the expected

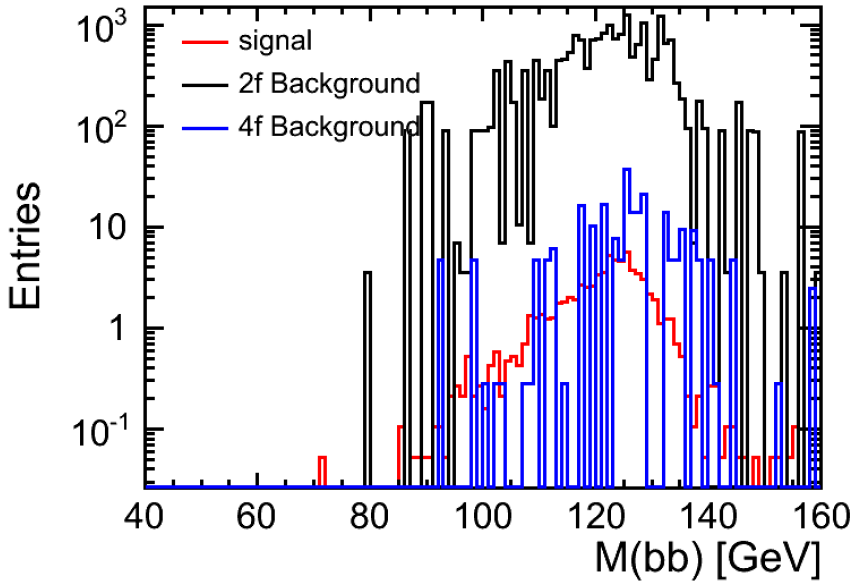

Figure 9: The distribution of $m(b\bar{b})$ after all the other cuts for the signal and background normalized to 2000 fb^{-1}

significance is 0.53σ, for SM signal process $e^+e^- \to hgamma$ using $h \to b\bar{b}$ channel. We give the 95 % confidence level upper limit for the cross section of $e^+e^- \to h\gamma$ which is calculated as Equation 5: $\sigma_{h\gamma}^{CL95} < 1.08$ fb, with 2000 fb^{-1} at $\sqrt{s} = 250$ GeV and left handed beam polarizations.

Table 2: The cut table

	Signal	background	Significance
Expected	237	3.14×10^8	0.01
Pre selection	222	6.54×10^7	0.02
b_{tag} $\geq$0.8	200	4.96×10^6	0.09
E_{mis} $\leq$35	182	4.30×10^6	0.09
$mvabdt \geq 0.0126$	75	1.98×10^4	0.53

$$\sigma = \frac{1.64}{\text{significance}}\sigma_{SM} \tag{5}$$

According to formula Equation 6, we can set the bound on the parameter $\zeta_A Z$.

$$3.09 > \frac{\sigma_{\gamma H}}{\sigma_{SM}} = 1 - 201\zeta_A - 273\zeta_{AZ} > 0 \ (assume\ \zeta_A = 0) \tag{6}$$

$$-0.0077 > \zeta_{AZ} > 0.0037 \tag{7}$$

5 Further Study

We are trying to improve the analysis by adding $h \to WW^*$ channel. The branching ratio of this channel is around 21% and created about 50 event. The main background We expect in this channel would be $e^+e^- \to W^+W^-$ with a hard ISR photon. In the $h \to b\bar{b}$ channel, the main background $e^+e^- \to b\bar{b}$ with a hard ISR photon is significantly enhanced due to radiative return to Z-pole. Hence we would expect a higher signal to background ratio in $h \to WW^*$ channel. Stay tuned.

Note in the next step when $h \to WW^*$ channel is completed, the experimental bound on ζ_{AZ} will also be translated into a bound on Dimension-6 operators.

6 Acknowledgement

We would like to thank the LCC generator working group and the ILD software working group for providing the simulation and reconstruction tools and producing the Monte Carlo samples used in this study. This work has benefited from computing services provided by the ILC Virtual Organization, supported by the national resource providers of the EGI Federation and the Open Science GRID.

References

[1] Ties Behnke et al., The International Linear Collider Technical Design Report - Volume 1: Executive Summary, arXiv:1306.6327v1 [physics.acc-ph]

[2] Shinya Kanemura,et al., Single Higgs production in association with a photon at electronpositron colliders in extended Higgs models, arXiv:1808.10268[hep-ph]

[3] TIan Junping,et al., Diphoton resonances at the ILC, Phys.Rev. D94 (2016) 095015

[4] Ties Behnke et al., The International Linear Collider Technical Design Report - Volume 4: Detec- tors, arXiv:1306.6329 (2013)[physics.ins-det]

[5] Physsim home page http://www-jlc.kek.jp/subg/offl/physsim/

[6] Wolfgang Kilian, Thorsten Ohl, Ju rgen Reuter, WHIZARD simulating multi-particle processes at LHC and ILC, Eur. Phys. J. C 71, 1742 (2011)

[7] Mokka Home page, http://ilcsoft.desy.de/portal/software$_packages/mokka/$

[8] S. Agostinelli et al. (GEANT4 Collaboration), Nucl. Instrum. Methods Phys. Res., Sect. A 506, 250 (2003).

[9] ILC Soft home page, http://ilcsoft.desy.de/portal

[10] M. Thomson, Nucl. Instrum. Methods Phys. Res., Sect. A 611, 25 (2009).

[11] LCFI+ home page https://confluence.slac.stanford.edu/display/ilc/LCFIPlus

[12] TMVA home page https://root.cern/tmva